THE JOURNAL OF BIOLOGICAL CHEMISTRY
Vol. 278, No. 28, Issue of July 11, pp. 25816–25824, 2003

Printed in U.S.A.

Type III Protein Translocase

HrcN IS A PERIPHERAL MEMBRANE ATPASE THAT IS ACTIVATED BY OLIGOMERIZATION*

Received for publication, February 24, 2003, and in revised form, April 21, 2003
Published, JBC Papers in Press, May 6, 2003, DOI 10.1074/jbc.M301903200

Charalambos Pozidis‡, Aggeliki Chalkiadaki‡, Amalia Gomez-Serrano, Henning Stahlberg§, Ian Brown¶, Anastasia P. Tampakaki, Ariel Lustig§, Giorgos Sianidis, Anastasia S. Politou‖, Andreas Engel§, Nickolas J. Panopoulos, John Mansfield¶, Anthony P. Pugsley, Spyridoula Karamanou, and Anastassios Economou‡‡**

*From the Institute of Molecular Biology and Biotechnology, FORTH and Department of Biology, University of Crete, P.O. Box 1527, GR-711 10 Iraklio, Crete, Greece, §M.E. Mueller Institute for Structural Biology, Biozentrum, University of Basel, Klingelbergstrasse 70, CH-4056 Basel, Switzerland, the ¶Department of Biological Sciences, Imperial College at Wye, University of London, Ashford, Kent, United Kingdom TN25 5AH, the ‖Laboratory of Biological Chemistry, Medical School, University of Ioaninna, Ioannina 45110 Greece, and the **Molecular Genetics Unit CNRS FRE 2364, Institut Pasteur, 25 Rue du Dr. Roux, 75724 Paris Cedex 15, France*

Type III protein secretion (TTS) is catalyzed by translocases that span both membranes of Gram-negative bacteria. A hydrophilic TTS component homologous to F_1/V_1-ATPases is ubiquitous and essential for secretion. We show that *hrcN* encodes the putative TTS ATPase of *Pseudomonas syringae* pathovar *phaseolicola* and that HrcN is a peripheral protein that assembles in clusters at the membrane. A decahistidinyl HrcN derivative was overexpressed in *Escherichia coli* and purified to homogeneity in a folded state. Hydrodynamic analysis, cross-linking, and electron microscopy revealed four distinct HrcN forms: I, 48 kDa (monomer); II, ~300 kDa (putative hexamer); III, 575 kDa (dodecamer); and IV, ~3.5 MDa. Form III is the predominant form of HrcN at the membrane, and its ATPase activity is dramatically stimulated (>700-fold) over the basal activity of Form I. We propose that TTS ATPases catalyze protein translocation as activated homo-oligomers at the plasma membrane.

Bacteria have evolved several protein translocases. One of these is the type III secretion (TTS)[1] apparatus of pathogenic and symbiotic bacteria (1). TTS translocases are related to bacterial flagella (2) and comprise at least 20 different subunits and auxiliary factors. TTS machines assemble from "stacks" of distinct substructures, each residing in one compartment of the bacterial envelope (2–8). Exported substrates are either diffusible polypeptides (*e.g.* toxins) or subunits of extracellular needle/pili-like appendages tethered to the cell surface (2). Secretion (9, 10) may take place through the hollow inside of TTS machines (~25-Å inner diameter) (7, 8, 11). Extracellular appendages contact the eucaryotic host cell surface and may facilitate toxin transport into the eucaryotic cytosol (1).

TTS translocases contain an inner membrane core (4, 12) and a putative ATPase that is essential for secretion and is related to F_1-ATPase subunits (13–15). However, whereas F_1-ATPase is functional as an $\alpha_3\beta_3$ hexamer, flagellar FliI was proposed to be monomeric (16, 17). FliI (18) and *Salmonella* InvC (15) have been shown to hydrolyze ATP, albeit at much lower levels than the F_1. Genetic and *in vitro* studies have suggested physical interactions between the ATPase and other TTS components (16, 17, 19, 20). Nevertheless, ultrastructural studies have failed to detect the ATPase associated with the TTS translocase (7, 8, 12, 21), and the structure, topology, and function of these proteins remain elusive.

To understand the molecular mechanism of the TTS ATPase, we purified and characterized HrcN of *Pseudomonas syringae* pathovar *phaseolicola*. HrcN is present in four quaternary forms. Of these, Form III (575 kDa) is a highly activated ATPase, a peripheral membrane protein, and may catalyze protein translocation.

EXPERIMENTAL PROCEDURES

Bacterial Strains and Plasmids—Escherichia coli strains and plasmids were manipulated as described (22, 23). *P. syringae phaseolicola* NPS3121 was grown at 30 °C in King's B medium (24) or *hrp*-derepressing fructose minimal medium (25) containing rifamycin (100 μg/ml).

The $hrcN_{Psph}$ coding sequence was PCR-amplified (Deep Vent DNA polymerase; New England Biolabs) using cosmid pPL6 (carrying the *P. syringae phaseolicola* TTS regulon) (26) as a template and oligonucleotide primers (forward) 5′-TGAGGTGAACATATGAACGCTGCACTGAGC-3′ and (reverse) 5′-GCGGATCGGATCCCAGTGTGTCTTCC-3′ tailed with *Nde*I and *Bam*HI restriction endonuclease sites, respectively. The *Nde*I-*Bam*HI fragment was cloned in the corresponding sites of pET16b, giving rise to pIMBB240.

Metal Affinity Chromatography—$His_{10}HrcN_{Psph}$ was purified by metal affinity chromatography. *E. coli* cells expressing HisHrcN (~36 g) were grown in LB medium (40 liters) supplemented with ampicillin (0.1 mg/ml) and IPTG (0.3 mM) for 3 h at 22 °C. Cells were harvested, resuspended in Buffer A (450 ml; 50 mM Tris-HCl, pH 8, 50 mM NaCl, 10 mM β-mercaptoethanol, 50 mM imidazole, 20% glycerol), and broken by sonication (8 × 30 s; 10-μm setting; 4 °C; Soniprep 150). Insoluble debris and membranes were removed by ultracentrifugation (100,000 × *g*; 4 °C) Cytosolic extracts were loaded at 1.5 ml/min on a Ni^{2+}-nitrilotriacetic acid Fast Flow (Qiagen) resin (30 ml; equilibrated with Buffer A). The resin was washed with Buffer A (4.5 liters), followed by 150 ml

* This work was supported by European Union Directorate of Science and Technology Grants Biotech2-BIO4-CT97-224 (to A. Ec., N. J. P., and J. M.) and RTN1-1999-00149 (to A. Ec., A. E., and A. P. P.), the a grant from the BBSRC (to J. M.), and the Maurice Mueller Foundation and Swiss National Foundation for Scientific Research Grant 31-59415.99 (to A. E.). The costs of publication of this article were defrayed in part by the payment of page charges. This article must therefore be hereby marked "*advertisement*" in accordance with 18 U.S.C. Section 1734 solely to indicate this fact.

The amino acid sequence of this protein can be accessed through NCBI Protein Database under NCBI accession number CAD22886.

‡ These authors contributed equally to this work.

‡‡ To whom correspondence should be addressed. Tel./Fax: 30-2810-391166; E-mail: aeconomo@imbb.forth.gr.

[1] The abbreviations used are: TTS, type III secretion; BN-PAGE, blue native PAGE; DSP, dithiobis(succinimidyl propionate); SEC, size exclusion chromatography; RZC, rate zonal centrifugation; TEM, transmission electron microscopy; IPTG, isopropyl-1-thio-β-D-galactopyranoside; FPLC, fast protein liquid chromatography; MOPS, 4-morpholinepropanesulfonic acid.

of Buffer A, 50 mM imidazole. Immobilized HisHrcN was eluted with two imidazole steps of 150 mM (~6 mg) and 350 mM (~24 mg).

Hydrodynamic Analyses—SEC was as described (22), using Superose 6HR 10/30 or Superdex 200HR 10/30 prepacked FPLC columns (Amersham Biosciences). Stoke's radii (R) were determined from a plot of K_{av} *versus* log R of standards (see Table I) as described (27). Elution volumes were converted to K_{av} by the equation $K_{av} = (V_e - V_o)/(V_t - V_o)$, where V_o represents the void volume (7.2 ml), V_t is the total bed volume (24 ml), and V_e is the elution volume. Sedimentation through sucrose gradients was carried out in a benchtop ultracentrifuge (Optima TLX; Beckman) (28). Typically, purified protein (20–40 μg or 200 μl of 10 mg/ml total cytoplasmic extract) was layered on a 2-ml 20–40% sucrose gradient prepared in 50 mM Tris-HCl, pH 8.0, 200 mM NaCl, 10 mM EDTA, 5 mM dithiothreitol. After centrifugation (14 h; 50,000 rpm; 210,000 × g; TLS-55 rotor), fractions (100 μl) were collected. Proteins separated by SDS-PAGE were visualized by Coomassie Brilliant Blue staining or by immunostaining. $s_{20,w}$ values were determined by their sedimentation relative to protein standards (see Table I).

M_r values were calculated as described (27). $M_r = [(s_{20,w}fN)/(1 - v\rho)]$, where f (frictional coefficient) = $6\pi\zeta R$, N is Avogadro's number, ζ is the solvent viscosity (of water) (1.0019 centipoise), R is the Stokes radius (meters), v is the protein's partial specific volume (0.74 ml/g) calculated from its amino acid composition (available on the World Wide Web at pbil.ibcp.fr), and ρ is the density of water (0.99823 g/ml).

AUC was performed on an Optima XL-A analytical ultracentrifuge (Beckman) equipped with a 12-mm Epon double-sector cell in an An-60 Ti rotor. Sedimentation equilibrium runs were performed at 20 °C. Average molecular masses were evaluated using a floating base-line computer program (SEGAL) that adjusts the base-line absorbance to obtain the best linear fit of ln(absorbance) *versus* the square of the radial distance as described (available on the World Wide Web at www.biozentrum.unibas.ch/personal/jseelig/AUC/software00.html). A partial specific volume of 0.73 ml/g was used.

Transmission Electron Microscopy—HisHrcN particles were adsorbed for 20 s to glow-discharged carbon-coated copper grids, washed three times in double-distilled water, and negatively stained with 0.75% uranyl formate. Images were recorded on Eastman Kodak Co. SO-163 film (nominal magnification × 50,000), using a Hitachi H-8000 transmission electron microscope operating at 200 kV and employing low dose conditions (5 electrons/A^2 per image).

To examine Hrp pilus production, *E. coli* strains were grown on TEM grids overnight in LB at 37 °C and washed twice in warmed LB, and cell density was adjusted to 0.2 A_{600} (29). IPTG (2 mM final concentration) was added, and 20-μl drops of the suspension were applied to TEM grids and incubated (5 h, 30 °C). Cells for sectioning were prepared as above except that they were grown in 10-ml flasks (5 h), pelleted, and fixed (1 h; 2% formaldehyde, 0.5% glutaraldehyde, 50 mM sodium cacodylate, pH 7.2), dehydrated in a graded ethanol series, and embedded in LR white resin. Ultrathin sections (90 nm) were mounted on 300-mesh gold grids and immunogold-labeled (29).

Chemicals, Biochemicals, and Miscellaneous Methods—Chemicals were from Sigma, DNA enzymes were from MINOTECH, oligonucleotides were from MWG, dNTPs were from Promega, Sequenase was from Amersham Biosciences, cross-linkers were from Pierce, Centricon ultrafiltration concentrators were from Millipore, and detergents were from Anatrace. Protein purification, manipulations, and detection were as described (22, 30), using Amersham Biosciences FPLC systems and columns. Blue native electrophoresis was as described (31). Inner membrane vesicles were prepared as described (32, 33).

RESULTS

Expression and Purification of HisHrcN—The gene for *P. syringae phaseolicola* HrcN was identified after systematic sequencing of the Hrp/Hrc regulon that encodes the TTS components.[2] Translation is predicted to initiate with a valine codon (Fig. 1*A*). $HrcN_{Psph}$ carries characteristic Walker box A and B sequences (Fig. 1*A*) required for ATP hydrolysis and is homologous to other putative TTS ATPases (34–36) and to F_1- and V_1-type ATPase subunits (23–25% identical and ~20% strongly similar residues). The protein is devoid of a Sec-system signal peptide and of extensive hydrophobic patches (Fig. 1*B*).

HrcN synthesized with an amino-terminal decahistidinyl tag in *E. coli* was purified to homogeneity (Fig. 1*C*, *lane 5*), and a polyclonal antiserum was raised against it (see "Experimental Procedures"). HisHrcN yield was poor (1 mg/liter); an expressed band of the expected molecular weight (48 kDa) was clearly detectable by α-HisHrcN immunostaining (*lanes 8* and *10*) and poorly by Coomassie Brilliant Blue staining (*lane 2*). A unique band of 48 kDa was also detected by α-HisHrcN immunostaining in extracts from *P. syringae phaseolicola* cells that had been induced for TTS expression (Fig. 2*D*, *lane 6*) (25) but not in extracts from uninduced cells (*lane 5*). The α-HrcN

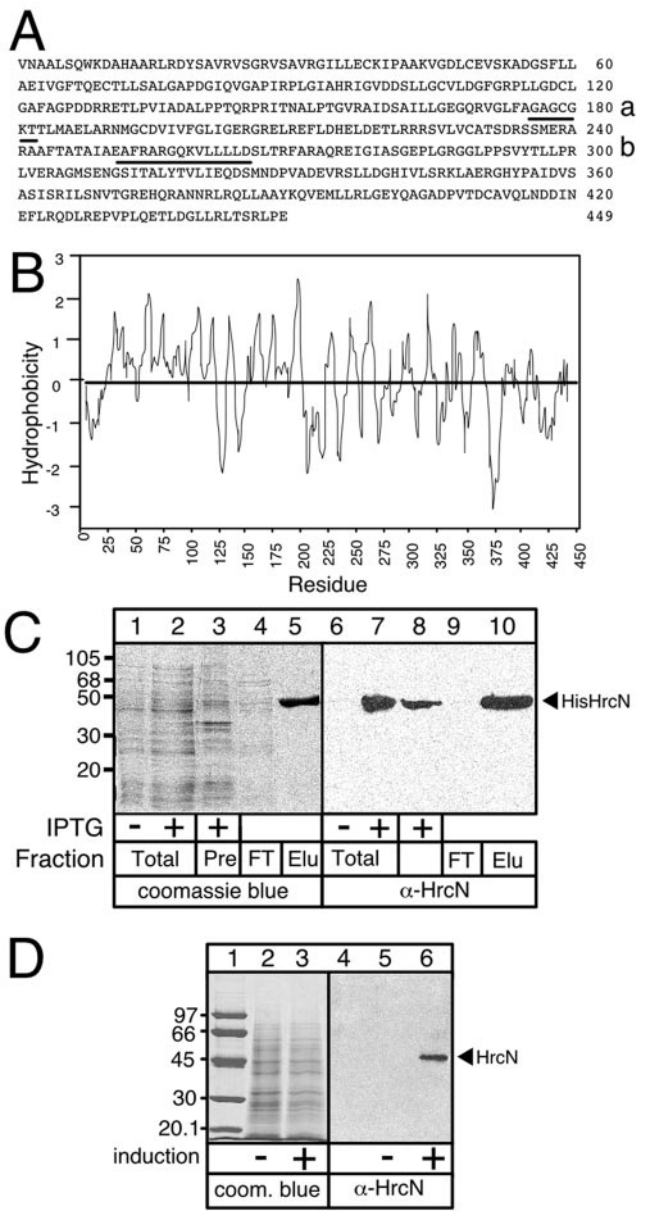

FIG. 1. **HisHrcN purification.** *A*, sequence of *P. syringae phaseolicola* HrcN. *a* and *b*, potential Walker boxes A and B (*underlined*). *B*, *P. syringae phaseolicola* HrcN "Kyte-Doolittle" hydropathicity plot (47) using a 9-residue window. Positive values represent increased hydrophobicity. *C*, HisHrcN purification. Cells of *E. coli* BL21/pLys/pIMBB240 at A_{600} = 0.5–0.6 were grown for a further 6 h in the absence or presence of IPTG (0.2 mM; 22 °C). HisHrcN was purified by metal affinity chromatography (see "Experimental Procedures"). Proteins were analyzed by SDS-PAGE and stained by Coomassie Brilliant Blue or α-HrcN immunostaining as indicated. Positions of M_r markers are indicated. *Pre*, preload cytosolic extract; *FT*, flow-through; *Elu*, affinity resin eluate. *D*, native *P. syringae phaseolicola* HrcN. Cells were grown in the presence (*lane 3*) or absence (*lane 2*) of TTS regulon expression (25). Polypeptides (30 μg) were analyzed as in *C*. *Lane 1*, M_r marker proteins.

[2] A. P. Tampakaki and N. J. Panopoulos, unpublished results.

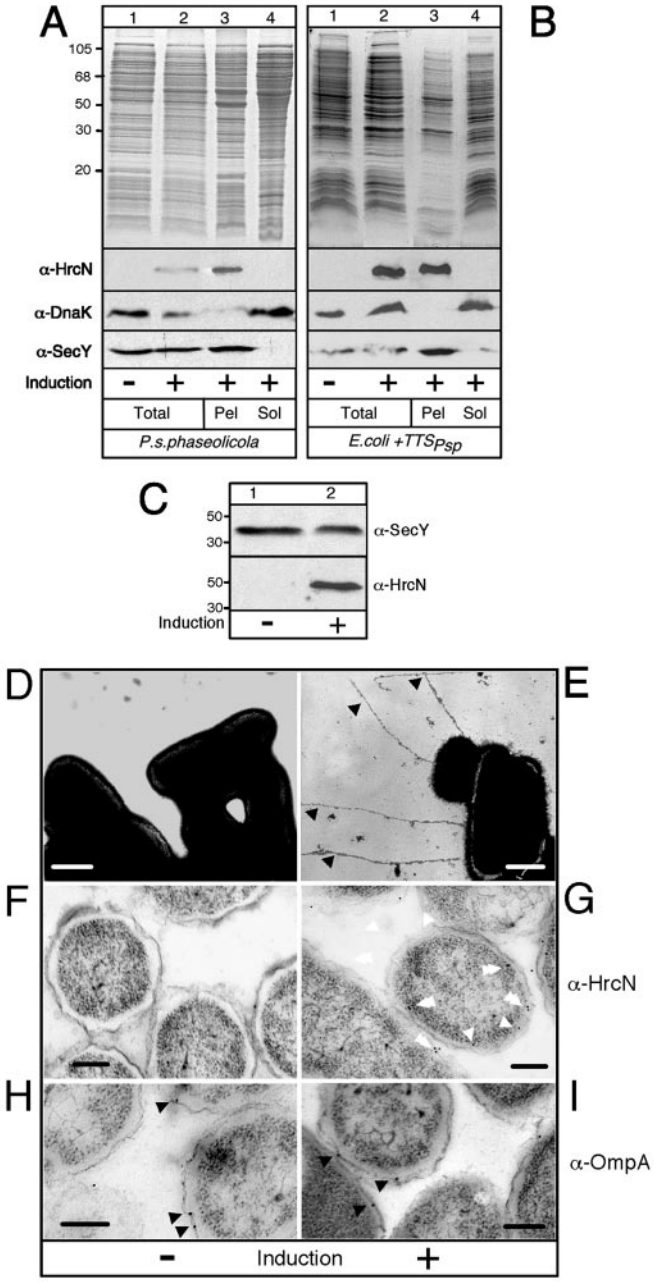

FIG. 2. **HrcN subcellular localization.** *A*, subcellular fractionation of HrcN-expressing cells. *P. syringae phaseolicola* cells were induced for TTS translocase expression (25) (*lanes 2–4*). Harvested cells were disintegrated by sonication. After debris removal (10,000 × *g* centrifugation) extracts were separated into the soluble fraction (*Sol*) and the insoluble membrane material (*Pel*) by ultracentrifugation (100,000 × *g*). Polypeptides (45 μg) were analyzed by SDS-PAGE and Coomassie Brilliant Blue (*upper panel*) and were immunostained as indicated. *B*, *E. coli* MC4100/pPPY430/pHrpL (23) cells were induced (0.5 mM IPTG) as indicated and analyzed as in *A*. *C*, *E. coli* MC4100/pPPY430/pHrpL cells were grown in the presence or absence of TTS induction as indicated. Inner membrane vesicles prepared from these cells were solubilized, and their polypeptides were analyzed by SDS-PAGE and α-HrcN or α-SecY immunostaining. M_r markers are indicated. *D* and *E*, micrographs of negatively stained *E. coli* MC4100/pPPY430/pHrpL grown on TEM grids in the presence or absence of TTS induction (5 h; 2 mM IPTG) as indicated. *Black arrowheads*, TTS pili. *Bars*, 1 μm. *F* and *G*, HrcN immunogold labeling. Thin sections of embedded *E. coli* MC4100/pPPY430/pHrpL cells grown as in *D* and *E*. Samples were treated with α-HrcN IgG (1:500 dilution) and anti-rabbit secondary antibody coupled to gold particles (*white arrows*). In bacteria induced for TTS expression, 20.35 gold particles per medial section of each bacterium ($n = 20$) were detected with most of the label occurring in clusters (*double white arrows*; 1.1 cluster per bacterial section). The envelope of the noninduced strain (*F*) is only weakly labeled (3.85 labels/section; $n = 20$), and there is no clustering. *Bars*, 0.25 μm. *H* and *I*, thin sections of embedded *E. coli* MC4100/pPPY430/pHrpL cells grown as in *D* and *E* immunogold labeled with α-pro-OmpA IgG (1:500 dilution; *black arrowheads*). *Bars*, 0.25 μm.

antiserum was used to subcellularly localize HrcN.

HrcN Associates with Membranes—To determine the subcellular localization of HrcN, we produced cytosolic extracts of *P. syringae phaseolicola* (Fig. 2*A*) grown under TTS regulon-inducing (*lanes 2–4*) or noninducing (*lane 1*) conditions and examined them by immunostaining. HrcN was only detected after growth under inducing conditions (*lane 2*), whereas two control proteins, DnaK and SecY, were expressed under both conditions. TTS-expressing cells were disrupted, and polypeptides were separated into soluble (*lane 4*) and membrane-associated (*lane 3*) material by ultracentrifugation (see "Experimental Procedures"). Most of HrcN (~90%) was detected in the membrane-containing fraction that also contains the polytopic membrane protein SecY (37). As expected, the cytoplasmic DnaK protein was almost exclusively detected in the soluble fraction. Similar results were obtained with *E. coli* MC4100 harboring the complete *P. syringae phaseolicola* TTS regulon on the low copy number cosmid pPPY430 and the *hrpL* σ factor under *lac* control on a separate plasmid (23, 38). MC4100/pPPY430/pHrpL grown in the presence (Fig. 2*B*, *lane 2*) but not in the absence (*lane 1*) of IPTG expressed HrcN. Intracellular HrcN production is coincident with biosynthesis of the extracellular TTS pilus (Fig. 2*E*, *arrows*) (9) and with the acquisition of pathogenic potential (data not shown) (23). TTS pili were not present in noninduced cells (Fig. 2*D*). As expected, expression of control proteins DnaK and SecY remained largely unaltered under both conditions (Fig. 2*B*). Fractionation of cellular material from induced cells revealed that HrcN is found predominantly in the insoluble membrane fraction together with SecY (*lane 3*), whereas DnaK is found in the soluble fraction (*lane 4*). To exclude the possibility that HrcN co-sediments with membranes through nonspecific aggregation, MC4100/pPPY430/pHrpL was grown in the presence (Fig. 2*C*, *lane 2*) and in the absence (*lane 1*) of IPTG, and inner membrane vesicles were prepared (32, 33). HrcN was isolated bound to inner membrane vesicles from cells expressing the TTS regulon (*lane 2*) but not from the nonexpressing cells (*lane 1*), whereas the inner membrane protein SecY was present on both vesicle preparations. In summary, our data indicate that HrcN appears to specifically associate with the inner membrane of the cell.

To further study HrcN membrane association, we performed α-HrcN immunogold labeling (Fig. 2, *F* and *G*). On whole cell thin sections, most (16-fold more) gold particles were localized specifically to the inner face of the cell envelope of *E. coli* MC4100 expressing the *P. syringae phaseolicola* TTS (Fig. 2*G*) rather than to the cytosol. Interestingly, most of the gold particles were clustered (Fig. 2*F*). Labeling was largely specific to HrcN, since 5-fold fewer gold particles localized to the cell envelope of cells that did not express the TTS regulon (Fig. 2*F*). Immunogold labeling of the major outer membrane protein A (OmpA) revealed a similar distribution of gold particles (95% of total label) to the cell periphery of both induced (Fig. 2*I*) and uninduced cells (Fig. 2*H*). 75–80% of the label localized specifically to the outer membrane leaflet. We conclude that HrcN associates with the inner membrane.

HrcN Is a Peripheral Membrane Protein—To examine the nature of HrcN association with the membrane, we employed a number of reagents used routinely to differentiate integral membrane proteins from peripherally associated polypeptides (Fig. 3). Even at modest concentrations, the chaotropes urea (Fig. 3*A*) and guanidine (Fig. 3*B*), efficiently removed HrcN

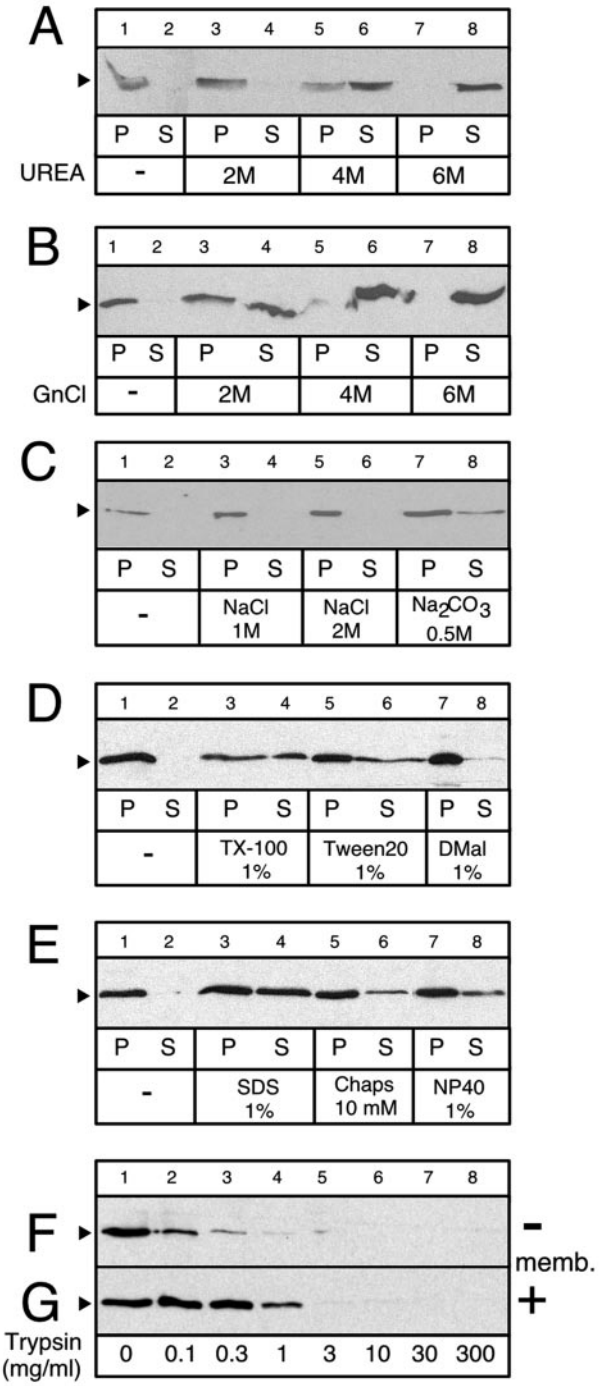

FIG. 3. **HrcN is a peripheral membrane protein.** *A–E* and *G*, membranes (20 μg of protein) from MC4100/pPPY430/pHrpL were treated with various reagents as indicated (30 min; 4 °C) and sedimented by ultracentrifugation. *DMal*, β-dodecyl maltoside. *F*, soluble HisHrcN and membrane-bound HrcN (15 ng) (*G*) were trypsinized (4 °C; 10 min). The reaction was stopped with 10 mM Pefabloc. All samples were analyzed by SDS-PAGE and α-HrcN immunodetection.

(Fig. 3, *lanes 4* and *6*), indicating that the protein is only peripherally associated with the membrane. Other agents removed membrane-bound HrcN less efficiently (Na_2CO_3; Fig. 3*C*, *lane 8*) or not at all (NaCl; *lanes 4* and *6*), suggesting that HrcN interaction with the membrane is strong. All of the detergents tested extracted and solubilized significant amounts of HrcN from the membrane (Fig. 3, *D* (*lanes 4* and *6*) and *E* (*lanes 4*, *6*, and *8*)), although dodecyl maltoside was less efficient (Fig. 3*D*, *lane 8*).

Finally, trypsinolysis was used to probe accessibility of HrcN at the membrane. Soluble HrcN is particularly sensitive to even low amounts of trypsin and appears by immunostaining with the polyclonal α-HrcN antiserum to be completely digested at trypsin concentrations above 0.1 μg/ml (Fig. 3*F*, *lanes 3* and *4*). Protease resistance of an equivalent amount of membrane-bound HrcN (Fig. 3*G*, *lane 1*) was significantly enhanced (compare *lanes 2–4* of *G* with *lanes 2–4* of *F*). Nevertheless, no immunostaining of the membrane-bound protein was detectable at trypsin concentrations above 3 μg/ml (Fig. 3*G*, *lane 5*), suggesting extensive degradation. Therefore, HrcN bound to the membrane is only partially protected and remains largely protease-accessible. We conclude that HrcN is a peripheral membrane protein that tightly associates with an unknown membrane component(s).

HisHrcN Is a Functional ATPase—Is HisHrcN a structurally intact and enzymatically active ATPase? Far UV CD showed that recombinant HisHrcN is folded and extensively α-helical (>40%; Fig. 4*A*) and melts in three distinct transitions ($Tm1_{app}$ = 41.3, $Tm2_{app}$ = 46, and $Tm3_{app}$ = 62.7 °C; Fig. 4*B*). This indicated that HisHrcN is structurally intact, and its ATPase function was tested below. HisHrcN hydrolyzes ATP in a linear time-dependent manner (Fig. 4*C*). Increasing the ATP concentration reveals that HisHrcN displays apparent Michaelis-Menten saturation kinetics (Fig. 4*D* and see below), yielding a V_{max} of 40 (μmol of P_i/mg of HisHrcN/min) and an apparent K_m of 1.3 mM. HisHrcN ATP hydrolysis was optimal in the presence of Mg^{2+} but not of other divalent metal ions (Fig. 4*E*), at pH 8 (Fig. 4*F*), and at 28 °C (Fig. 4*G*). Interestingly, HisHrcN ATPase activity was stimulated by increased protein concentration in a nonlinear fashion (Fig. 4*H*), suggesting that the enzyme may be cooperatively activated by self-association (see below). We conclude that HisHrcN is a highly active ATPase that may be activated by homo-oligomerization.

HisHrcN Oligomerization—F_1- and V_1-ATPases are hexameric (39, 40). To examine whether HisHrcN also oligomerizes, we investigated its hydrodynamic behavior using size exclusion chromatography (SEC; Fig. 5*A*) and rate zonal centrifugation (RZC; Fig. 5*B*). SEC analysis on a Superose 6 resin (exclusion limit >5 MDa; Fig. 5*C*) revealed four HisHrcN populations with distinct Stokes radii (Table I): Form I (fractions 39–48) presumably monomeric and the most prominent species (~82%); Form II (fractions 36–39); Form III (fractions 26–34); and Form IV (fractions 19–21). Form II (see Fig. 5*A*; 150 mM elution) was not always detectable and could not be studied further. Form III, the second most prominent (~13%), migrated as a broad peak, suggesting a dynamic assembly state.

We next examined HisHrcN quaternary organization using RZC (Fig. 5*B*; see "Experimental Procedures") (28). HisHrcN Form IV and a mixture of Forms I–III were analyzed separately in 20–40% sucrose gradients. The four forms migrated as distinct species with defined sedimentation coefficients (Table I). Sedimentation coefficients (determined by RZC) were combined with Stokes radii (determined by SEC) to provide molecular weights irrespective of shape (Table I; see "Experimental Procedures") (27). These indicate that Form I corresponds to a HisHrcN monomer ($M_{r(app)}$ = 46,700). Form II ($M_{r(app)}$ = ~300,000) could represent hexamers, and Form III ($M_{r(app)}$ = 570,000–714,000) could represent dodedamers or slightly larger homo-oligomers (Table I). Form IV is a very large species ($M_{r(app)}$ ~3.8 MDa).

To accurately measure the masses of the HisHrcN forms, we employed sedimentation equilibrium analytical ultracentrifugation. Scaling up of HisHrcN purification yielded amounts sufficient for analytical ultracentrifugation analysis only of Forms I and III (Fig. 5*C*; Table I). A single exponential curve optimally fitted to the available data revealed calculated masses for Form I and III of 43.5 kDa (monomer) and 575.8

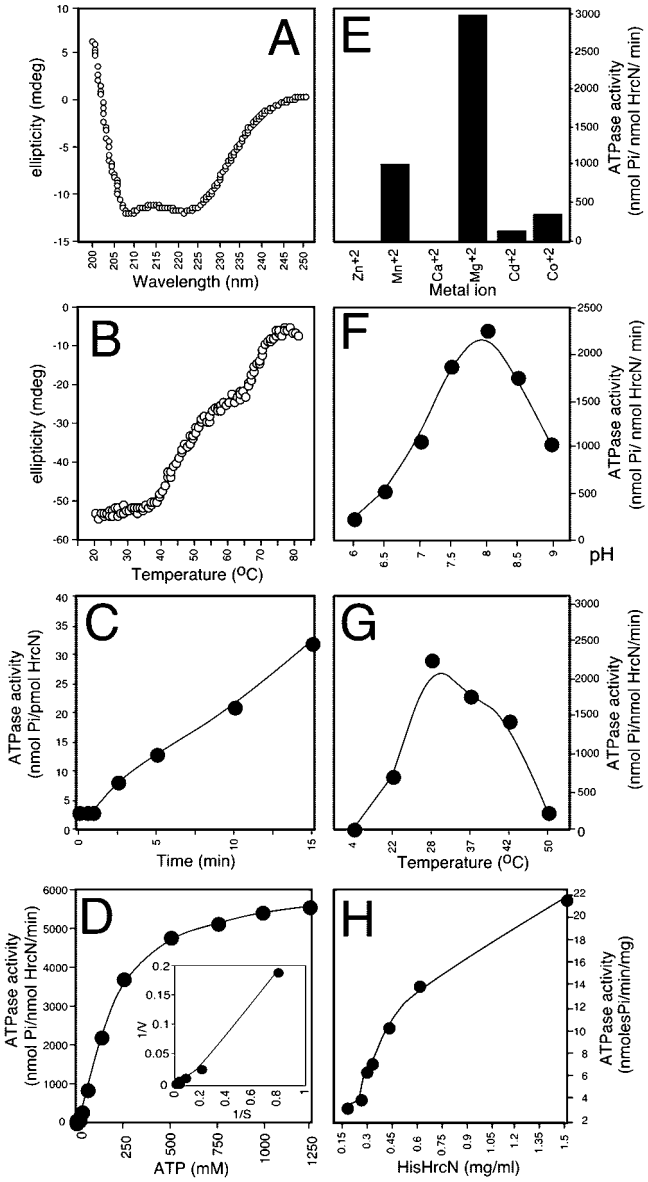

FIG. 4. **HrcN secondary structure and ATPase activity.** *A*, HisHrcN secondary structure. Far UV CD spectra (190–255 nm) were determined at ambient temperature as described (22). *B*, HisHrcN thermal denaturation. Ellipticity determined by far UV CD (222 nm) as described (30). HisHrcN (200 μl, 200 μg/ml in 5 mM MOPS buffer, pH 7.5, 5 mM $MgCl_2$) was heated at 50 °C/h. *C–H*, ATP hydrolysis by HisHrcN (20 μg/ml) (*A*, *C–E*) determined by measuring phosphate release (10 min at 30 °C) (30) in buffer B (50 mM Tris-Cl, pH 8, 50 mM KCl, 5 mM MgCl, 200 mg/ml bovine serum albumin) unless otherwise indicated. *C*, time course of HrcN ATP hydrolysis. *D*, Michaelis-Menten kinetics at the indicated ATP concentrations. V_{max} and K_m values were determined as described (22). *E*, optimal metal co-factor requirement. The indicated cations were at 5 mM. *F*, pH dependence. pH was stabilized at 6–7 with HEPES-KOH and 7.5–9 with Tris-Cl buffers. *G*, temperature dependence of the ATPase activity. *H*, concentration dependence of the ATPase activity.

kDa (11.9 subunits), respectively.

HisHrcN Form III from the peak SEC fraction of Fig. 5*A* was also examined by negative stain transmission electron microscopy (Fig. 5*D*). Peak fraction 30 contained a distribution of fairly uniform particles (*white arrows*). Image averaging (*inset*) reveals a round particle with 13 ± 1-nm outer diameter. Additional less uniform particles are also seen in the micrograph (*black arrows*). These particles are very large and presumably represent material aggregated during adsorption on the grid. We conclude that HisHrcN oligomerizes into homo-hexa- and dodecameric assemblies in solution in the absence of ligands or other TTS proteins.

HisHrcN Form III Is a Highly Active ATPase—To determine whether all forms of HisHrcN were active in ATP hydrolysis, SEC fractions of HisHrcN were assayed for ATPase activity (Fig. 6*A*). Strikingly, the bulk of the high level ATPase activity was associated with Form III despite the fact that Form III represents only a minor physical population of the enzyme. In contrast, the activity of Form I, the major HisHrcN population, was measurable albeit low. ATPase activities of Forms II and IV were very low and were not studied further.

To compare the activities of Forms I and III, we characterized the chromatographic peak fractions by detailed kinetics (Table II). Form I had a K_m of 0.1 mM, whereas that of Form III was 10-fold higher. Form I had a low ATP turnover similar to that of other TTS ATPases (15, 18). Strikingly, the specific activity (*i.e.* ATP turnover per protomer) of Form III was more than 700 times that of Form I (Table II).

To exclude the possibility that the ATPase activity associated with Form III was the result of a highly active contaminant present in trace amounts, we sought to determine whether Form III could be assembled *de novo* from isolated monomeric HisHrcN. To this end, highly purified HisHrcN Form I (see "Experimental Procedures") largely devoid of Form III (<2%) was concentrated (as in Fig. 4*H*), and samples at increasing concentrations were analyzed by SEC (Fig. 6*B*). Concentration caused visible reduction of Form I and concomitant increase of Form III. Similarly, the ATPase of Form III generated in this experiment is also enhanced significantly in a concentration-dependent manner (Fig. 6*C*) and displays a specific ATP turnover (33 min^{-1}/protomer) similar to that of unconcentrated Form III (Table II).

We conclude that the HisHrcN ATPase is hyperactivated upon dodecamerization, implying that Form III is a physiologically relevant form of the enzyme and does not arise from nonspecific aggregation. Form III may be the functional form of the enzyme during TTS protein translocation.

Native Soluble P. syringae phaseolicola HrcN Forms Oligomers—To test whether native HrcN in *P. syringae phaseolicola* is also oligomeric, we first characterized HrcN from the small cytoplasmic pool. Cytosolic polypeptides from *P. syringae phaseolicola* expressing the TTS translocase were cross-linked *in vivo* (Fig. 7*A*). The addition of the homobifunctional amine-specific cross-linker DSP led to the appearance of two novel slow migrating species with approximate masses of ~300 and ~600 kDa (*lane 2*; *filled arrows*) not present in the untreated sample (*lane 1*). Both cross-linked species disappeared upon reduction of the cross-linker (*lane 3*). Two nonspecific immunoreacting cytosolicpolypeptides that are not affected by DSP were used as internal controls (*lane 2*; *open arrows*). Similar results were obtained with formaldehyde (data not shown).

We next determined whether the cross-linked species (Fig. 7*A*) derived from preexisting HrcN oligomers. Polypeptides from TTS-expressing *P. syringae phaseolicola* cells were separated by SEC (Fig. 7, *B* and *C*) and RZC (Fig. 7, *D* and *E*), analyzed by SDS-PAGE, and visualized by either Coomassie Brilliant Blue (Fig. 7, *B* and *D*) or by α-HrcN immunostaining (Fig. 7, *C* and *E*). Four distinct HrcN forms were identified: Form I, monomeric HrcN (Fig. 7*E*, *fractions 4–8*); Form II of ~300 kDa (Fig. 7*E*; *fractions 11* and *12*), Form III of ~629 kDa (Fig. 7*C*, *fractions 33–35*, and Fig. 7*E*, *fractions 14* and *17*), and Form IV of ~3.5 MDa (Fig. 7*C*, *fractions 18–21*, and Fig. 7*E*, *fractions 19* and *22*). The ratio between the four forms varied in different cell extracts, perhaps implying a dynamic assembly state.

We conclude that, like recombinant HisHrcN, native HrcN

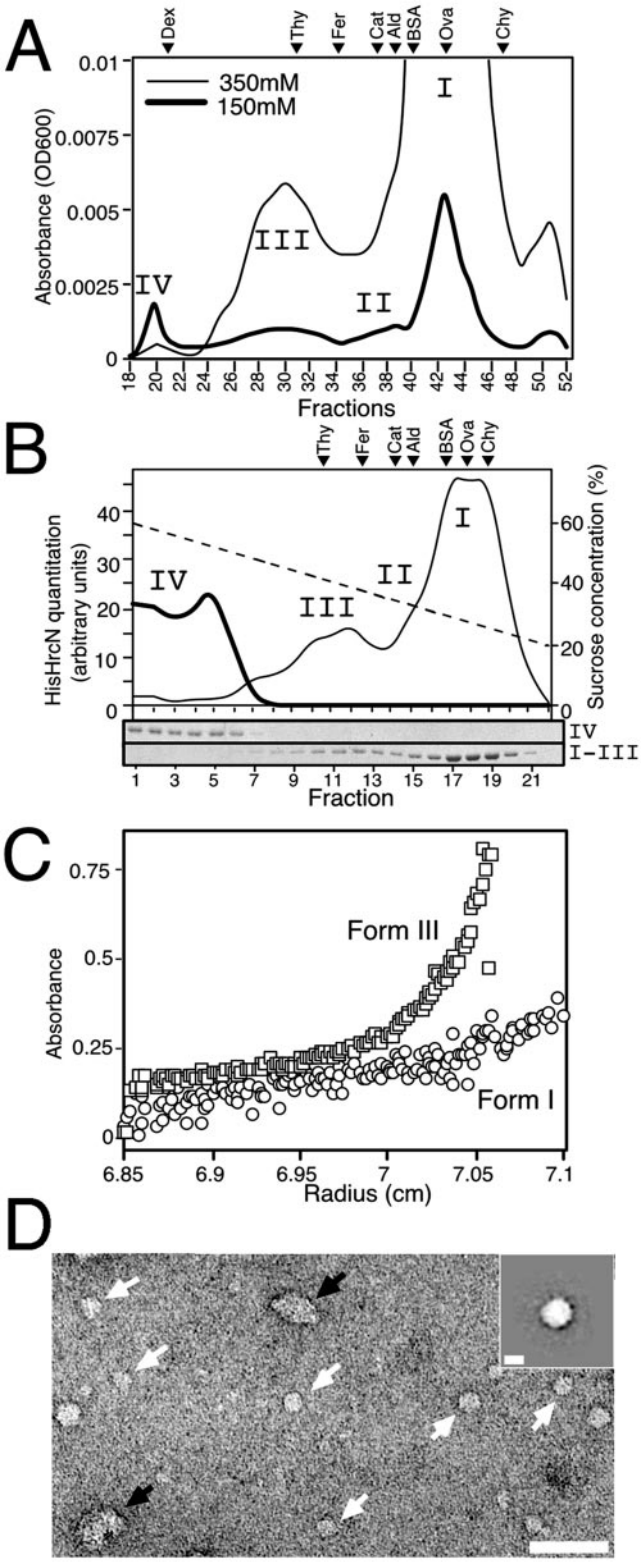

FIG. 5. **HisHrcN oligomers.** *A*, HisHrcN SEC (see "Experimental Procedures"). HisHrcN was eluted from a Ni^{2+} affinity resin with either 150 mM imidazole (which allows visualization of Form II) or 350 mM (which enriches for Forms I and III). HisHrcN was subsequently chromatographed on Superose 6 (*B*) (0.25 mg/ml), and fractions (0.4 ml) were collected. Four HisHrcN forms (*latin numerals*) were resolved and detected by online absorption (280 nm; *solid line*; arbitrary units). *Dex*, blue dextran (~2 MDa); for other markers, see Table I. *B*, HisHrcN RZC. Form IV (*thick line*) or a mixture of Forms I–III (*fine line*) of HisHrcN (50–120 μg in 200 μl) purified by SEC were analyzed individually by RZC sucrose gradients (20–40%; 2 ml). Fractions (22 × 100 μl) were carefully removed from the top of the gradient. A portion of each fraction (80 μl) was precipitated by trichloroacetic acid (15%, 20 min, 4 °C), collected by centrifugation, and analyzed by SDS-PAGE followed by α-HrcN immunostaining (*bottom*). Band intensities were quantitated by scanning densitometry and superimposed on the plot. Migration positions of marker proteins centrifuged during the same run on identical gradients but in separate tubes are shown. *C*, sedimentation equilibrium. Individually purified His HrcN Forms I and III (1.2 mg/ml; 50 mM Tris-Cl, 200 mM NaCl, and 5 mM β-mercaptoethanol) were analyzed by analytical ultracentrifugation at 18,000 (Forms I) and 6,400 (Form III) rpm (detection at 279 nm), and molecular masses were determined as described (see "Experimental Procedures"). *D*, TEM analysis. HrcN Form III (0.2–0.6 mg/ml) from *A* was adsorbed to carbon-coated grids and stained with uranyl formate (see "Experimental Procedures"). *Scale bar*, 50 nm. *Inset*, reference-free alignment and averaging of 77 particles using the SPIDER program (48). *Scale bar*, 10 nm.

forms oligomeric assemblies *in vivo* in the *P. syringae phaseolicola* cytoplasm. These assemblies have apparent masses similar to the four forms of purified HisHrcN (Fig. 5, Table I) and may represent hetero- or homo-oligomers.

Native HrcN at the Membrane Is Dodecameric—To determine which of the HrcN forms is membrane-bound (Figs. 2 and 3), isolated membranes from TTS-expressing *E. coli* were treated with the homobifunctional cysteine-specific cross-linker bismaleimidohexane (*BMH*; Fig. 8*A*) to promote the formation of interprotomer covalent links between the nine HrcN cysteinyl residues. A gradual increase of the cross-linker concentration from 0.03 mM (*lane 2*) to 0.36 mM (*lane 5*) led to the appearance of discreet higher order species of ~300 and ~600 kDa followed by the disappearance of the monomeric form. Similar results were obtained using the cross-linker DSP (Fig. 8, *lanes 6–8*).

To examine oligomerization of membrane-bound HrcN under more "native" conditions and to determine its mass, BN-PAGE (31) was employed (Fig. 8*B*). Isolated membranes from TTS-expressing *E. coli* were extracted with the nonionic detergent β-octyl glucoside, and solubilized polypeptides were separated by BN-PAGE and immunostained with α-HrcN antibodies. A single broad band of ~600 kDa was detected in these extracts (Fig. 8*B*, *lane 2*) but was not present in extracts from noninduced cells (*lane 1*). Since the same migration behavior was seen at different detergent concentrations (0.25–2%), including those below the critical micellar concentration, the detergent is unlikely to contribute excessively to the apparent mass. This ~600-kDa membrane-extracted HrcN species migrates similarly to the soluble dodecameric HisHrcN Form III (Fig. 8*B*, *lane 3*). In addition, BN-PAGE analysis reveals the presence of a distinct ~150-kDa species (*filled arrow*) not seen previously with the other methods. These results indicate that the dodecamer is the predominant membrane-bound HrcN form.

DISCUSSION

We have initiated the mechanistic and energetic characterization of the TTS translocase using the *P. syringae phaseolicola* TTS as a model system. Here we demonstrate that HrcN is a high level ATPase that is activated by oligomerization and associates peripherally with the membrane.

HisHrcN was purified in a folded form and in amounts sufficient for biochemical and structural analysis. The protein melts in three transitions, which could indicate that HrcN, like the F_1-ATPase subunits (40), is a three-domain protein. Hydrodynamic, cross-linking, and ultrastructural analyses revealed that both native HrcN and recombinant HisHrcN assemble in distinct quaternary forms (Fig. 5–8; Table I): (*a*) a monomeric Form I of ~48 kDa; (*b*) a rather unstable Form II of ~300 kDa that could be a transient intermediate (Form II may be similar to the X-300 cross-linked species (Figs. 7*A* and 8*A*); (*c*) the dodecameric 575-kDa Form III that comprises an organized round particle with an outer diameter of ~13 nm (Fig. 5*D*) (this

TABLE I
Hydrodynamic analysis of HrcN

HisHrcN was produced in *E. coli,* whereas native HrcN is synthesized in *P. syringne pnaseolicola* (25). Values for marker proteins (thyroglobulin, ferritin, catalase, aldolase, BSA, ovalbumin, and chymotrypsinogen A) were from Amersham Biosciences. SEC, size exclusion chromatography; RZC rate zonal centrifugation; AUC, analytical ultracentrifugation. Combination of SEC + RZC was according to Ref. (27). ND, not determined Values represent averages of three experiments

Protein	Stokes radius (*R*)	Sedimentation coefficient (*s*)	HrcN native molecular mass	
			SEC + RZC	AUC
	nm	10^{-13} *s*	*K Da*	
HisHrcN (I)	3.12 ± 0.15	3.2 ± 0.15	46.7 ± 1.6	43.7 ± 1.2
HisHrcN (III)	9.6 ± 0.5	14.5 ± 1.4	626 ± 78	575.8 ± 23.1
HisHrcN (IV)	31.4 ± 1.8	27.8 ± 1.1	3,830 ± 580	ND
HrcN (I)	ND	ND	48 ± 2	ND
HrcN (III)	7.9 ± 0.9	18.3 ± 0.8	629 ± 36	ND
HrcN (IV)	25.7 ± 1.2	31.1 ± 1.1	3,470 ± 390	ND

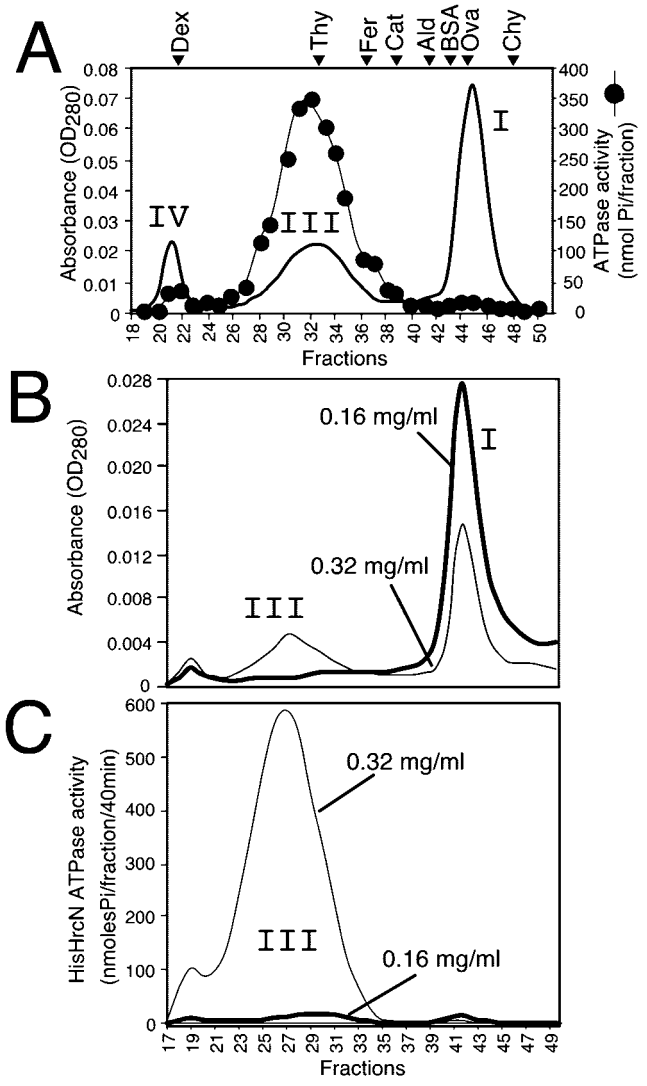

FIG. 6. **HisHrcN Form III is a hyperactivated ATPase.** *A*, HisHrcN SEC. HisHrcN was chromatographed as in Fig. 5*A*. The ATPase activity of a portion of the fractions (50–200 μl) was determined (*filled circles*). *B*, SEC (as in Fig. 5*A*) of monomeric HisHrcN (0.16 mg/ml) purified from a Ni^{2+}-nitrilotriacetic acid resin and of the same material concentrated (0.32 mg/ml) by ultrafiltration. *C*, ATPase activities of SEC fractions from *B* analyzed as in *A*.

particle, with an average protein density of 0.8 Da/Å^3 and an assumed height of 5.6 nm, would have the mass of Form III in solution (~575 kDa)); and (*d*) Form IV, a very large aggregate (Table I). An additional form of 150 kDa was only detected by BN-PAGE (Fig. 8*B*). Concentration of HisHrcN Form I leads to *de novo* formation of Form III (Fig. 6, *B* and *C*) in a reversible

TABLE II
Steady state ATPase kinetics of HisHrcN Forms I (monomer) and III (dodecamer) determined as described (30)

Specific activities are calculated as turnover numbers (K_{cat}) per protomer. Values represent averages of four experiments.

HisHrcN	ATP hydrolysis			
	K_M	V_{max}	K_{cat}	K_{cat} (*protomer*)
	mM	*mmol PI/mgHrcN/min*	s^{-1}	s^{-1}
Form I	0.114 ± 0.01	0.0635 ± 0.003	0.052 ± 0.003	0.052 ± 0.003
Form III	1.3 ± 0.13	43 ± 1.6	447 ± 21	37.3 ± 1.1

reaction.[3] Therefore, since oligomerization does not require any detectable auxiliary factors, it is an intrinsic property of the HrcN polypeptide. The findings that Form III is active in ATP hydrolysis (Fig. 6), is obtained in the presence of reducing agent, forms canonical particles (Fig. 5*D*), and is also generated natively in wild type *P. syringae phaseolicola* cells (Fig. 7) argue strongly against the possibility that the dodecameric particle is the result of nonspecific aggregation or misfolding. Nevertheless, it will be important to accurately determine the kinetics of assembly-disassembly of the "ATPase-inactive" monomer to the "ATPase-active" dodecameric particle. Modulation of this reaction may be a fundamental element of the catalytic cycle.

Immunogold localization (Fig. 2*G*) and biochemical fractionation (Figs. 2, *A–C*, and 3) experiments revealed that ~90% of HrcN associates with the membrane. Importantly, membrane-bound HrcN is almost exclusively a dodecamer (Fig. 8*B*). It was recently suggested that the homologous FliI ATPase may associate with the phospholipid component of the cell membrane (41). Earlier studies failed to demonstrate a direct physical link of the TTS ATPase with the membrane where the putative translocation "conduit" resides. Other ATPases that catalyze protein translocation through membranes (*e.g.* Tim44 (42), PulE (43), and SecA (37)) are also soluble proteins that associate peripherally albeit very tightly with membranes. We are currently examining the potential role of lipids or proteinaceous factors (*e.g.* other TTS subunits) in HrcN membrane assembly. Such composite interactions would explain three distinct properties of HrcN observed here: (*a*) it is relatively recalcitrant to extraction from the membrane with agents (other than nonchaotropes) that usually remove peripheral membrane proteins (Fig. 3*C*); (*b*) its ATPase activity in solution is unregulated (Table I); and (*c*) immunoelectron microscopy experiments reveal a significant degree of clustering at defined membrane locations (Fig. 2*G*). Such sites could represent associations of dodecameric HrcN with the membrane-embedded TTS translocase. Other soluble, peripheral ATPase subunits of

[3] C. Pozidis and A. Economou, unpublished results.

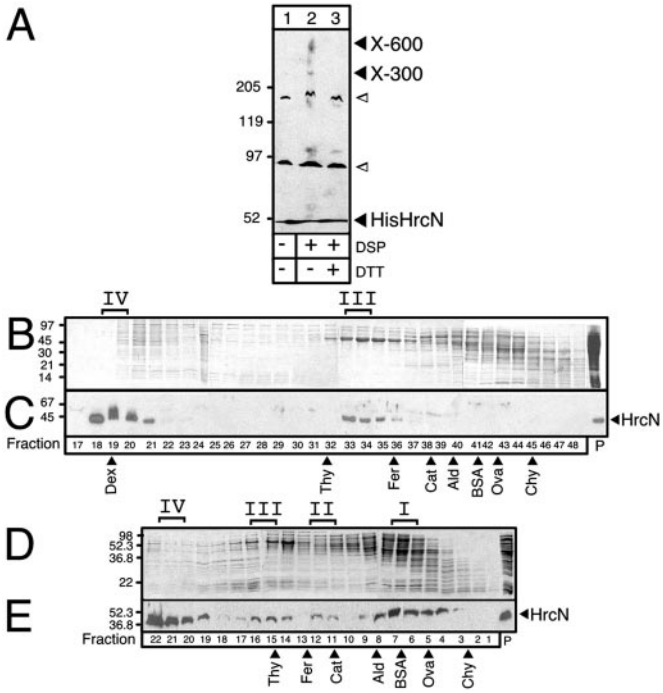

FIG. 7. **Cross-linking and hydrodynamic analysis of *P. syringae phaseolicola* HrcN.** *A*, *in vivo* cross-linking. Synthesis of the *P. syringae phaseolicola* TTS translocase was induced for 14 h (25). The cells were harvested at A_{600} = 0.8–1.0 and washed in 50 mM Hepes, pH 7, and aliquots (50 μl) were incubated with DSP (2 mM, 30 min, 25 °C). The reaction was stopped with 1 M Tris-Cl, pH 8. Cells were harvested, and polypeptides were analyzed (as in Fig. 1*D*). *X-300* and *X-600*, cross-linked species; *open arrows*, internal control polypeptides. *B* and *C*, SEC of *P. syringae phaseolicola* cytosol. Cytosolic extracts (800 μg of total protein in 200 μl) of *P. syringae phaseolicola* expressing TTS translocase were analyzed by SEC (0.4-ml fractions). The polypeptides were harvested, analyzed by SDS-PAGE (30 μg of total protein/lane), and stained by Coomassie Brilliant Blue (*B*) or by α-HrcN immunostaining on Western blots (*C*). Distinct HrcN forms are indicated (*latin numerals*). *P*, preload material. *D* and *E*, HrcN sedimentation analysis. Cytosolic extracts (as in *A*) were analyzed by RZC (as in Fig. 5*B*). *P*, preload material.

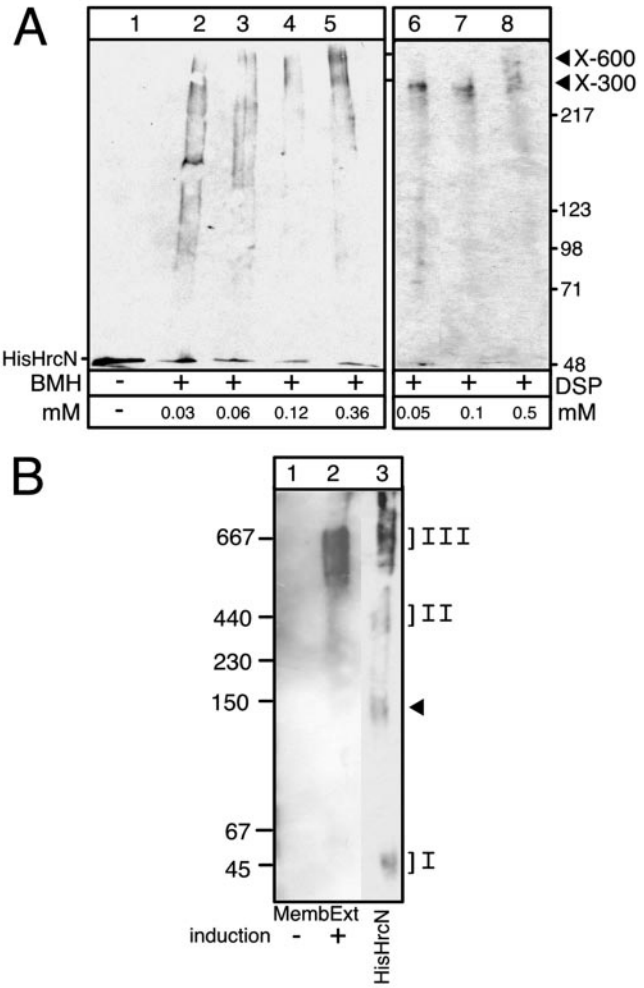

FIG. 8. **Membrane-bound HrcN is oligomeric.** Membranes (45 μg of protein) of MC4100/pPPY430/pHrpL expressing *P. syringae phaseolicola* TTS were isolated and treated with the following. *A*, bismaleimidohexane (*BMH*) (4 °C, 30 min) or DSP (24 °C, 30 min) at the indicated amounts. Cross-linked polypeptides were analyzed by SDS-PAGE and detected by α-HrcN immunostaining. *B*, β-octyl glucoside (1% (w/v); 4 °C, 30 min; *lanes 1* and *2*; *MembExt*), separated by BN-PAGE (31), and detected by α-HrcN immunostaining. HisHrcN (*lane 3*) was purified as in Fig. 1*C*. M_r markers are as in Table I.

protein translocases (*e.g.* SecA) (37) are similarly tightly bound to the membrane with complex lipid and protein interactions and appear to even become integrated in the bilayer plane.

Mutagenesis experiments and sequence conservation between TTS (14, 15) and flagellar ATPases (13) and the F_1/V_1-ATPase subunits suggested that these proteins may link metabolic energy to secretion through the TTS translocase. HisHrcN has at least two distinct ATPase activities: the low level basal activity of monomeric HisHrcN (K_{cat} = 0.052 s^{-1}) (Table II) that is similar to the ATPase activities of a *Shigella* InvC-glutathione *S*-transferase fusion (K_{cat} = 0.2 s^{-1}) (15) and of the flagellar FliI (K_{cat} = 0.16 s^{-1}) (18) and the novel high level activity of HisHrcN Form III (K_{cat} = 37.3 s^{-1}) (Table II). In fact, there is a cooperative induction of the ability of the enzyme to hydrolyze ATP as it assembles from Form I into Form III (Figs. 4*H* and 6, *B* and *C*). Similarly, assembled F_1 hexamers detached from the membrane component (F_0) are highly active in ATP hydrolysis (40), whereas individual $F_1\beta$ or α monomers are not (44). In F_1 and several other ATPases, α/β dimers form the minimal mononucleotide binding and ATPase unit (44). Our data indicate that oligomerization of the TTS ATPase may act as an intramolecular regulatory activation mechanism.

Aditional intermolecular factors may control the activation of HrcN ATPase by regulating its oligomerization. One such factor could be the FliH protein (HrpE in *P. syringae phaseolicola*; YscL in *Yersinia*), shown to bind to the flagellar TTS ATPase FliI (19, 20) *in vitro* and to repress the basal ATPase activity of monomeric FliI (16). Thus, FliI, which, like HrcN, interacts with itself (19), may be prevented from forming large oligomeric assemblies (16, 17) active in ATP hydrolysis. Such interactions would ensure that the active dodecameric form of the TTS ATPase is only assembled in a controlled and ordered manner during the catalytic cycle at the membrane.

The observation that different HrcN forms can coexist (Figs. 5*A*, 7*E*, and 8*B*, *lane 3*) suggests that HrcN oligomerization is highly dynamic. This could explain why stable complexes of TTS machineries that include the ATPase have not yet been isolated. In this sense, TTS ATPases may be more similar to the dynamically assembling V_1 (39) rather than to the more stably membrane-bound F_1 (39, 40). F_1/V_1-ATPases function as hexamers of alternating $\alpha_3\beta_3$ subunits (39, 40) and, like HrcN, display ATPase activity in the absence of any other subunits (45). However, our experiments suggest that HrcN Form III has a dodecameric or two-hexamer organization. HrcN organization is therefore distinct from that of the F_1-ATPase. Other dodecameric traffic ATPases homologous to F_1 are known and comprise double hexameric stacks (AAA family) (46). HrcN Form II of ~300 kDa (Figs. 5*A*, 7, *A* and *E*, and 8*A*) that is

barely active in ATP hydrolysis (Fig. 6*A*) could represent a hexameric assembly intermediate.

Collectively, our data lead us to formulate the hypothesis that HrcN Form III may be the active enzyme species in the cell during TTS protein secretion. Clearly, additional experimentation using a functionally reconstituted *in vitro* system will be required to directly test this and to determine the physiological relevance of the other TTS ATPase forms. Determination of the molecular features that allow the apparently similar F_1 and TTS ATPases to participate in the transmembrane pumping of such divergent substrates (*i.e.* protons for the F_1/V_1 and polypeptides for the TTS) promises to be an exciting future challenge.

Acknowledgments—We are grateful to S. Müller for communicating data prior to publication; K. Tokatlidis and A. Kuhn for comments; K. Tokatlidis for help with BN-PAGE; V. Galanopoulos, E. Michelidaki, D. Bolis, K. Boulias, and C. Meesters for preliminary experiments; and G. Tsiamis for strains.

REFERENCES

1. Cornelis, G. R., and Van Gijsegem, F. (2000) *Annu. Rev. Microbiol.* **54,** 735–774
2. Macnab, R. M. (1999) *J. Bacteriol.* **181,** 7149–7153
3. Kubori, T., Matsushima, Y., Nakamura, D., Uralil, J., Lara-Tejero, M., Sukhan, A., Galan, J. E., and Aizawa, S. I. (1998) *Science* **280,** 602–605
4. Kimbrough, T. G., and Miller, S. I. (2000) *Proc. Natl. Acad. Sci. U. S. A.* **97,** 11008–11013
5. Tamano. K., Aizawa, S., Katayama, E., Nonaka, T., Imajoh-Ohmi, S., Kuwae, A., Nagai, S., Sasakawa, C. (2000) *EMBO J.* **19,** 3876–3887
6. Plano, G. V., Day, J. B., and Ferracci, F. (2001) *Mol. Microbiol.* **40,** 284–293
7. Sekiya, K., Ohishi, M., Ogino, T., Tamano. K., Sasakawa, C., and Abe, A. (2001) *Proc. Natl. Acad. Sci. U. S. A.* **98,** 11638–11643
8. Blocker, A., Jouihri, N., Larquet, E., Gounon, P., Ebel, F., Parsot, C., Sansonetti, P., and Allaoui, A. (2001) *Mol. Microbiol.* **39,** 652–663
9. Jin, Q., and He, S. Y. (2001) *Science* **294,** 2556–2558
10. Li, C. M., Brown, I., Mansfield, J., Stevens, C., Boureau, T., Romantschuk, M., and Taira, S. (2002) *EMBO J.* **21,** 1909–1915
11. Katayama, E., Shiraishi, T., Oosawa, K., Baba, N., and Aizawa, S. (1996) *J. Mol. Biol.* **255,** 458–475
12. Kubori, T., Sukhan, A., Aizawa, S. I., and Galan, J. E. (2000) *Proc. Natl. Acad. Sci.* **97,** 10225–10230
13. Dreyfus, G., Williams, A. W., Kawagishi, I., and Macnab, R. M. (1993) *J. Bacteriol.* **175,** 3131–3138
14. Woestyn, S., Allaoui, A., Wattiau, P., and Cornelis, G. R. (1994) *J. Bacteriol.* **176,** 1561–1569
15. Eichelberg, K., Ginocchio, C. C., and Galan, J. E. (1994) *J. Bacteriol.* **176,** 4501–4510
16. Minamino, T., and MacNab, R. M. (2000) *Mol. Microbiol.* **37,** 1494–1503
17. Minamino, T., Tame, J. R., Namba, K., and Macnab, R. M. (2001) *J. Mol. Biol.* **312,** 1027–1036
18. Fan, F., and Macnab, R. M. (1996) *J. Biol. Chem.* **271,** 31981–31988
19. Minamino, T., and MacNab, R. M. (2000a) *Mol. Microbiol.* **35,** 1052–1064
20. Jackson, M. W., and Plano, G. V. (2000) *FEMS Microbiol. Lett.* **186,** 85–90
21. Rossier, O., Van den Ackerveken, G., and Bonas, U. (2000) *Mol. Microbiol.* **38,** 828–838
22. Karamanou, S., Vrontou, E., Sianidis, G., Baud, C., Roos, T., Kuhn, A., Politou, A., and Economou, A. (1999) *Mol. Microbiol.* **34,** 1133–1145
23. Mansfield, J., Jenner, C., Hockenhull, R., Bennett, M. A., and Stewart, R. (1994) *Mol. Plant Microbe Interact.* **7,** 726–739
24. King, E. O., Ward, M. K., and Raney, D. E. (1954) *J. Lab. Clin. Med.* **44,** 301–307
25. Huynh, T. V., Dahlbeck, D., and Staskawitz, B. J. (1989) *Science* **245,** 1374–1377
26. Rahme, L. G., Mindrinos, M. N., and Panopoulos, N. J. (1991) *J. Bacteriol.* **173,** 575–586
27. Siegel, L. M., and Monty, K. J. (1966) *Biochim. Biophys. Acta* **112,** 346–362
28. Tanese, N. (1997) *Methods* **12,** 224–234
29. Brown, I. R., Mansfield, J. W., Taira, S., Roine, E., and Romantschuk, M. (2001) *Mol. Plant Microbe Interact.* **14,** 394–404
30. Sianidis, G., Karamanou, S., Vrontou, E., Boulias, K., Repanas, K., Kyrpides, N., Politou, A. S., and Economou, A. (2001) *EMBO J.* **20,** 961–970
31. Schagger, H., and von Jagow, G. (1991) *Anal. Biochem.* **199,** 223–231
32. Chang, C. N., Model, P., and Blobel, G. (1979) *Proc. Natl. Acad. Sci. U. S. A.* **76,** 1251–1255
33. Douville, K., Price, A., Eichler, J., Economou, A., and Wickner, W. (1995) *J. Biol. Chem.* **270,** 20106–20111
34. Lidell, M. C., and Hutcheson, S. W. (1994) *Mol. Plant Microbe Interact.* **7,** 488–497
35. Bogdanove, A. J., Wei, Z. M, Zhao, L., and Beer, S. V. (1996) *J. Bacteriol.* **178,** 1720–1730
36. Alfano, J. R., Charkowski, A. O., Deng, W. L., Badel, J. L., Petnicki-Ocwieja, T., van Dijk, K., and Collmer, A. (2000) *Proc. Natl. Acad. Sci. U. S. A.* **97,** 4856–4861
37. Economou, A. (2002) *Mol. Membr. Biol.* **19,** 159–169
38. Puri, N., Jenner, C., Bennett, M., Stewart, R., Mansfield, J., Lyons, N., and Taylor, J. (1997) *Mol. Plant Microbe Interact.* **10,** 247–256
39. Kane, P. M. (2000) *FEBS Lett.* **469,** 137–141
40. Yoshida, M., Muneyuki, E., and Hisabori, T. (2001) *Nat. Rev. Mol. Cell. Biol.* **2,** 669–677
41. Auvray, F., Ozin, A. J., Claret. L., and Hughes, C. (2002) *J. Mol. Biol.* **318,** 941–950
42. Neupert, W., and Brunner, M. (2002) *Nat. Rev. Mol. Cell. Biol.* **3,** 555–565
43. Possot, O., and Pugsley, A. P. (1994) *Mol. Microbiol.* **12,** 287–299
44. Kagawa, Y., Ohta, S., Harada, M., Kihara, H., Ito, Y., and Sato, M. (1992) *J. Bioenerg. Biomembr.* **24,** 441–445
45. Gromet-Elhanan, Z. (1992) *J. Bioenerg. Biomembr.* **24,** 447–452
46. Dalal, S., and Hanson, P. I. (2001) *Cell* **104,** 5–8
47. Kyte, J., and Doolittle, R. F. (1982) *J. Mol. Biol.* **157,** 105–132
48. Frank, J., Radermacher, M., Penczek, P., Zhu, J., Li, Y., Ladjadj, M., and Leith, A. (1996) *J. Struct. Biol.* **116,** 190–199